A path out of COVID-19 quarantine: an analysis of policy scenarios

Lia Humphrey[a], Edward W. Thommes[b], Roie Fields[a], Naseem Hakim[c], Ayman Chit[d], and Monica G. Cojocaru[a]

[a]Department of Mathematics and Statistics, University of Guelph, Guelph, Ontario, Canada; [b]Vaccine Epidemiology and Modeling, Sanofi Pasteur, Toronto, Ontario, Canada; [c]Founder, covid-testing.org; [d,1]Head Medical International, Sanofi Pasteur, Dalla Lana School of Public Health, University of Toronto, Canada

This manuscript was compiled on April 23, 2020

In this work we present an analysis of the two major strategies currently implemented around the world in the fight against COVID-19: Social distancing & shelter-in-place measures to protect the susceptible, and testing & contact-tracing to identify, isolate and treat the infected. The majority of countries have principally relied on the former; we consider the examples of Italy, Canada and the United States. By fitting a disease transmission model to daily case report data, we infer that in each of the three countries, the current level of national shutdown is equivalent to about half the population being under quarantine. We demonstrate that in the absence of other measures, scaling back social distancing in such a way as to prevent a second wave will take prohibitively long. In contrast, South Korea, a country that has managed to control and suppress its outbreak principally through mass testing and contact tracing, and has only instated a partial shutdown. For all four countries, we estimate the level of testing which would be required to allow a complete exit from shutdown and a full lifting of social distancing measures, without a resurgence of COVID-19. We find that a "brute-force" approach of untargeted universal testing requires an average testing rate of once every 36 to 48 hours for every individual, depending on the country. If testing is combined with contact tracing, and/or if tests are able to identify latent infection, then an average rate of once every 4 to 5 days is sufficient.

Pandemic modelling | Pandemic forecasting under policy | Testing frequency policy modelling |

1. Introduction

In late 2019, a novel betacoronavirus called SARS-CoV-2 emerged from a live animal marketplace in Wuhan, Hubei Province, China, and has since inflicted a worldwide pandemic of a disease now referred to as COVID-19. The disease appears to be highly contagious, with a suspected R_0 between 2.2 and 4.6 ((1),(2)) although it is important to consider that R_0 is not strictly biologically determined but rather heavily influenced by host behavioural and environmental factors ((3)). The incubation period has been found to be 5.1-5.2 days, while 97.5% of patients display symptoms within 11.5 days ((1),(4)). The disease spreads primarily through the respiratory tract and respiratory secretions, but recent evidence of COVID-19 in the blood and fecal matter of infected patients suggests other possible modes of transmission (5), (6).

As of April 19, 2020, there have been a total of 2.16 million confirmed cases of COVID-19 worldwide, and 146,000 deaths (WHO COVID-19 Situation Report 89, https://www.who.int/emergencies/diseases/novel-coronavirus-2019/situation-reports). All outbreaks apart from that of Hubei Province continue to be active, with new cases reported daily, though some countries, principally South Korea and Italy, have clearly passed a (first) peak. With few exceptions, countries have taken drastic social distancing measures (e.g. (7–10)) in an effort to suppress the disease, or at least prevent it from overwhelming a country's critical care capacity. However, these measures have had a massive effect on daily lives and economies throughout the world, and are clearly unsustainable. It is thus critical to devise strategies which will allow the phasing out of social distancing measures while preventing a resurgence of outbreaks ((10),(11)).

In this work, we fit a disease transmission model to daily case reports in order to assess the net effectiveness of the COVID-19 countermeasures that have been taken in different countries. We begin with the examples of Italy, Canada and the United States, three countries which have relied principally on social distancing via universal shelter-in-place measures. We demonstrate that the rate at which these measures can be eased while preventing future outbreaks is prohibitively slow. We compare these scenarios to that of South Korea, a country which has successfully controlled COVID-19 principally through highly aggressive testing and contact tracing, while maintaining a comparatively normal operating of society. We show that an analogous strategy provides a feasible path back to normalcy in Italy, Canada, the US, and by extension other countries.

The structure of the paper is as follows: In Section 2 we introduce our model main ideas, notation, and assumptions. We follow in Section 3 with the presentation of results for Italy, Canada, the US and South Korea, wherein we infer the net effect to date of social distancing (in the three former) and

Significance Statement

We demonstrate how current quarantine measures can be lifted after the current pandemic wave by large-scale, frequent-testing and contact tracing on the remaining susceptible populations. We present an analysis of the two major strategies currently implemented around the world against COVID-19: Social distancing & shelter-in-place measures to protect the susceptible, and testing & contact-tracing to identify, isolate and treat the infected. We find that a "brute-force" approach of untargeted universal testing requires an average testing rate of once every 36 to 48 hours for every individual, depending on the country. If testing is combined with contact tracing, and/or if tests are able to identify latent infection, then an average rate of once every 4 to 5 days is sufficient.

All authors contributed to the paper equally, from inception, model implementation to data fitting and forecast.

Edward W. Thommes and Ayman Chit are employees of Sanofi Pasteur. Monica G. Cojocaru has received national research grants in the past in which Sanofi Pasteur was a matching partner.

[2]To whom correspondence should be addressed. E-mail: mcojocar@uoguelph.ca

testing plus contact tracing (in the latter). We then evaluate scenarios for countries to phase out social distancing while preventing a resurgence of COVID-19 outbreaks. We present conclusions in Section 5. Additional mathematical background is included in Appendix A.

2. Materials and methods

A. The SQEIRL model. The transmission of an infectious disease in a homogeneously mixed population is often described by a Susceptible-Infectious-Recovered (SIR) model (12) or its variants, most notably a Susceptible-Exposed-Infectious-Recovered (SEIR); see (13) for a recent review. A SEIR model normalized to population size N is described by 4 differential equations of the form:

$$\begin{aligned} \frac{ds}{dt} &= -\beta si \\ \frac{de}{dt} &= \beta si - \sigma e \\ \frac{di}{dt} &= \sigma e - \gamma i \\ \frac{dr}{dt} &= \gamma i \end{aligned}$$

with $s = \frac{S}{N}$, $e = \frac{E}{N}$, $i = \frac{I}{N}$, $r = \frac{R}{N}$, $s+e+i+r = 1$ and where β is the rate of effective contacts, $1/\sigma = T_{lat}$ is the mean latent period (which may differ from the incubation period), and $1/\gamma = T_{inf}$ is the mean duration of infectiousness, with both times having exponential distributions. We also have the auxiliary equation for the cumulative number of cases,

$$\frac{dc}{dt} = \sigma e$$

The daily incidence of cases on day i is then

$$inc_i = c_i - c_{i-1}$$

In turn, a SIR model is similar to (1) but without the E compartment, thus only 3 differential equations subject to $s + i + r = 1$.

The spread of an infectious disease can be halted if its effective reproduction number

$$R_{eff} = R_0 s, \qquad [1]$$

can be decreased below 1. The effective reproduction number of both the SIR and SEIR compartmental disease transmission models is

$$R_{eff} = \frac{\beta}{\gamma} s. \qquad [2]$$

In both the SIR and SEIR model, when $s \approx 1$ and we are near the disease-free equilibrium $(1, 0, 0, 0)$, the early growth of both i and inc is exponential (see e.g. (13)):

$$i(t) = i_0 e^{\rho t}, inc(t) = inc_0 e^{\rho t} \qquad [3]$$

In the SIR model, the growth factor ρ is given by

$$\rho_{SIR} = \beta - \gamma = \gamma(R_0 - 1), \qquad [4]$$

One then can express R_0 in terms of ρ:

$$R_{0SIR} = \frac{\rho_{SIR} + \gamma}{\gamma} \qquad [5]$$

In a similar manner, in the SEIR model we have (13):

$$\rho_{SEIR} = \frac{-(\sigma + \gamma) + \sqrt{(\sigma - \gamma)^2 + 4\sigma\beta}}{2}. \qquad [6]$$

and by solving for β from Equation 6 we get:

$$R_{0SEIR} = \frac{(\rho_{SEIR} + \sigma)(\rho_{SEIR} + \gamma)}{\sigma\gamma}. \qquad [7]$$

In the limit as $\sigma \to \infty$, the SEIR model reduces to the SIR model, and accordingly, as can readily be shown by L'Hospital's rule:

$$\lim_{\sigma\to\infty} = \frac{(\rho_{SEIR} + \sigma)(\rho_{SEIR} + \gamma)}{\sigma\gamma} = \frac{\rho_{SIR} + \gamma}{\gamma} \qquad [8]$$

For COVID-19, as for other pandemics (e.g. SARS, MERS, the 1918 Spanish flu), we can assume the entire population to be initially susceptible. Therefore, in the early stages of an outbreak, $R_{eff} \approx R_0$. We will also assume that infection with COVID-19 confers subsequent immunity, which does not wane significantly over the time horizon considered here. Thus, whether they die or recover, an infected person is considered removed from the pool of susceptibles. In the absence of a vaccine or other control measures, $s(t) = 1 - c(t)$, where $c(t)$ is the cumulative number of people infected at time t.

From Equation 2, assuming β to be given, we see that R_{eff} can be decreased in two ways: by decreasing s at a rate higher than that due to infection alone; or by increasing γ. The former can be considered an abstraction of social distancing measures, since these effectively take a part of the population "out of circulation" as far as disease transmission is concerned. The latter can be achieved by identifying and isolating infected individuals early, thus cutting short T_{inf}.

To explicitly depict the role of control measures, we adapt the SEIR model to a pandemic setting by adding a Quarantined (Q) and an isoLated (L) compartment. As before, we include the auxiliary equation for C, the cumulative number of infected. The resulting SQEIRL model, a variant of a model introduced by Brauer (14) in the context of SARS, is described by:

$$\begin{aligned} \frac{ds}{dt} &= -\beta si - \alpha s + \epsilon q \\ \frac{dq}{dt} &= \alpha s - \epsilon q \\ \frac{de}{dt} &= \beta si - \sigma e - \kappa_1 e \\ \frac{di}{dt} &= \sigma e - (\gamma + \kappa) i \\ \frac{dr}{dt} &= \gamma i \\ \frac{dl}{dt} &= \kappa i + \kappa_1 e \\ \frac{dc}{dt} &= \sigma e \end{aligned}$$

where as in the standard SEIR model, β is the mean rate of effective contacts, $1/\sigma = T_{lat}$ is the mean latent period, and $1/\gamma = T_{inf}$ is the mean infectious period. Additionally, $1/\alpha = T_{quar}$ is the mean time for susceptibles to be quarantined—where "quarantined" constitutes an abstraction of social distancing measures—and $1/\epsilon = T_{return}$ is the mean time for people to leave quarantine. Finally, $1/\kappa_1 = T_{isol,lat}$ and $1/\kappa = T_{isol,inf}$ are the mean times for the latent and

infectious, respectively, to be isolated as a consequence of either testing or contact tracing.

For simplicity, we will consider changes in q to occur instantaneously at discrete times rather than continuously, so that between changes the system evolves as if there were no q compartment; we denote this form a S(Q)EIRL model. Its effective reproduction number is then given by (see Appendix A)

$$R_{eff,S(Q)EIRL} = s\frac{\beta\sigma}{(\sigma+\kappa_1)(\gamma+\kappa)} \quad [9]$$

It can be shown (see Appendix A) that the exponential growth rate (Equation 3) of infected near the disease-free equilibrium is

$$\rho_{S(Q)EIRL} = \frac{-(\sigma+\kappa_1+\gamma+\kappa)}{2} + \frac{\sqrt{((\sigma+\kappa_1)-(\gamma+\kappa))^2+4\sigma\beta s}}{2},$$

and the rate of effective contacts is

$$\beta_{S(Q)EIRL} = \frac{(\sigma+\kappa_1+\rho_{S(Q)EIRL})(\gamma+\kappa+\rho_{S(Q)EIRL})}{\sigma}$$

We can also express the effective reproduction number in terms of $\rho_{S(Q)EIRL}$:

$$R_{0S(Q)EIRL} = \frac{(\sigma+\kappa_1+\rho_{S(Q)EIRL})(\gamma+\kappa+\rho_{S(Q)EIRL})}{(\gamma+\kappa)\sigma}$$

3. Results

A. Estimating R_0 from early exponential growth. While growth is still exponential, we have from (Equation 3) that

$$\log(inc(t)) \propto \rho t \quad [10]$$

i.e. a log-linear plot of incidence versus time will have slope ρ. Indeed, early exponential growth can be seen to be a near-universal feature in COVID-19 daily case count data from around the world. Figures 1 and 2 plot $\log(inc)$ versus time for South Korea, Italy, Canada and the US, using time series data of daily new cases compiled by the Johns Hopkins University Center for Systems Science and Engineering (JHU CSSE) (15), retrieved from http://github.com/CSSEGISandData/COVID-19/tree/master/csse_covid_19_data

In all four countries the initial linear phase is clearly apparent, followed by a transition to sub-exponential growth. This transition is sharpest for South Korea, where growth switches abruptly to decay around 1 March. Regression fit results for ρ and the corresponding doubling time,

$$T_{dbl} = \frac{\ln(2)}{\rho} \quad [11]$$

together with dates for the onset of major national-level protective measures are given in Figures 1 and 2 and Table 1. In all four cases, the transition to sub-exponential growth occurred at or after the time that widespread protective measures were first invoked.

Inferring R_0 from ρ requires choosing values for the mean latent and infectious periods. The sum of these is the mean serial interval:

$$T_{ser} = T_{lat} + T_{inf} = \sigma^{-1} + \gamma^{-1} \quad [12]$$

Estimates of the serial interval of COVID-19 range from 3.95 to 6.6 days(16–19). We adopt a value of $T_{ser} = 5$ days. The latent period of the disease is not well constrained, but it can be shown (Appendix A) that for a given value of T_{ser} and ρ, the maximum value of R_0 is obtained when $T_{lat} = T_{inf} = T_{ser}/2$. We assume this "worst-case" scenario and let $T_{lat} = T_{inf} = 2.5$ days.

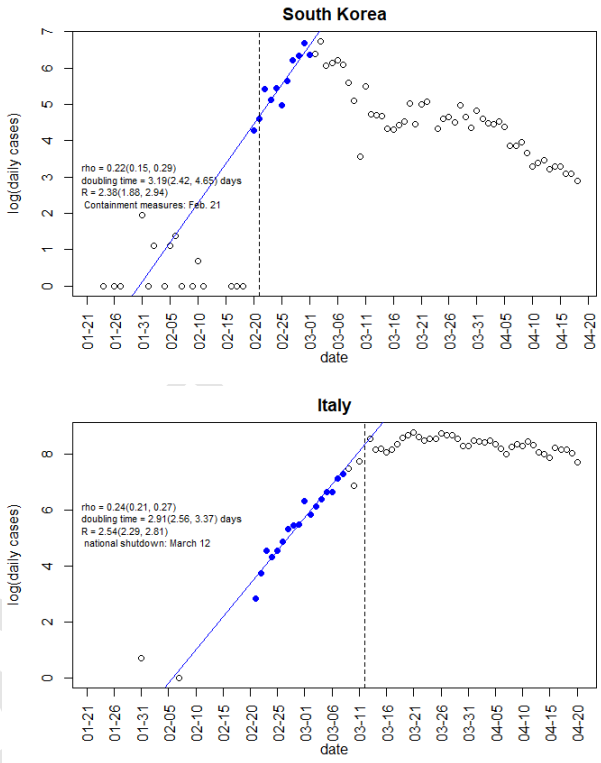

Fig. 1. Log-linear plots of daily COVID-19 incidence versus time for South Korea and Italy. The initial linear phase corresponds to exponential growth, which subsequently turns over into sub-exponential growth. The exponential growth factor ρ and the corresponding doubling time are estimated via a regression fit to the initial phase. A value for R_0 is calculated using Equation 9, and assuming $\sigma = \gamma = (2.5d)^{-1}$.

Country	ρ initial growth	R_0	
S. Korea	0.22(0.15,0.29)	2.38(1.88,2.94)	
Italy	0.24(0.21,0.27)	2.54(2.29,2.81)	
Canada	0.23(0.19,0.26)	2.45(2.20,2.72)	
US	0.33(0.30,0.36)	3.34(3.07,3.63)	
	counter-measures	sub-exponential onset	under-reporting factor
S. Korea	Feb 21(20)	March 1	0.69
Italy	March 12 (21)	March 22	0.058
Canada	March 20 (22)	April 3	0.31
US	March 13 (23)	April 6	0.16

Table 1. Summary of country-specific values for South Korea, Italy, the US and Canada. Estimates of initial exponential growth rate ρ are obtained from regression fits to the early phases of the outbreaks (Figures 1 and 2). Corresponding values of R_0 are calculated assuming $T_{lat} = T_{inf} = 2.5$ days. Estimates of under-reporting factors are taken from (24).

B. Quantifying the intensity of COVID-19 countermeasures thus far in Italy, Canada and the US. We begin with Italy,

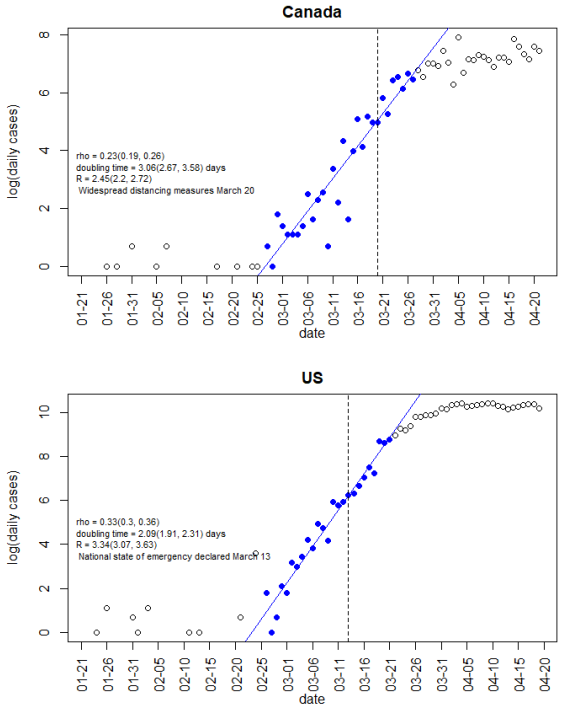

Fig. 2. As Figure 1, but for Canada and the US.

Canada and the US, three countries which have enacted social distancing via nationwide shutdowns and shelter-in-place orders. In Italy, the measures were ordered and coordinated country-wide, in Canada most provinces enacted similar measures over the course of 1-2 weeks around March 20, 2020, while the United States has had a more heterogeneous spread of similar measures, depending on specific states. We interpret the transition to sub-exponential growth (Figures 1 and 2) as the first signature of the effect of these measures in a given country, and use this as the starting point to infer the net effect that these measures have had up to April 19, 2020.

For each country, we fit the S(Q)EIRL model solutions for daily incidence $\{inc_{model,1}, ..., inc_{model,n}\}$ to daily case reports. The model output is multiplied by a factor kf, where k is an estimate of the fraction of symptomatic cases reported, obtained using delay-adjusted case fatality rates (24), and f is the fraction of cases which are symptomatic, estimated to be 0.5 from from a widespread testing campaign conducted in Iceland (25). We compute $-\log\mathcal{L}$, the normal negative log likelihood of the time series of observed daily incidences, $\{inc_{obs,1}, ..., inc_{obs,n}\}$, given the model output, as a function of model parameters

$$x = (i_0, q_1, q_2, ..., q_m)$$

where i_0 is the initial number of infected and the q_i are the fractions of susceptibles residing in the Q compartment each week, starting on the sub-exponential onset date of each country (see Table 1). R_0 for each country is fixed at the respective values obtained via regression above. Sets of parameters are drawn using unweighted (uniform) Latin hypercube sampling. The single best-fit solution is the one which minimizes $\mathcal{L}$. We estimate the 95% confidence interval as comprising all solutions having $-\log\mathcal{L} \leq (-\log\mathcal{L})_{min} + 1.92$ (see e.g. (26))

Figures 3 to 6 show the fitted solutions, the percentage of susceptibles needing to be effectively under quarantine each by week to produce the fits, and the corresponding effective reproduction numbers.

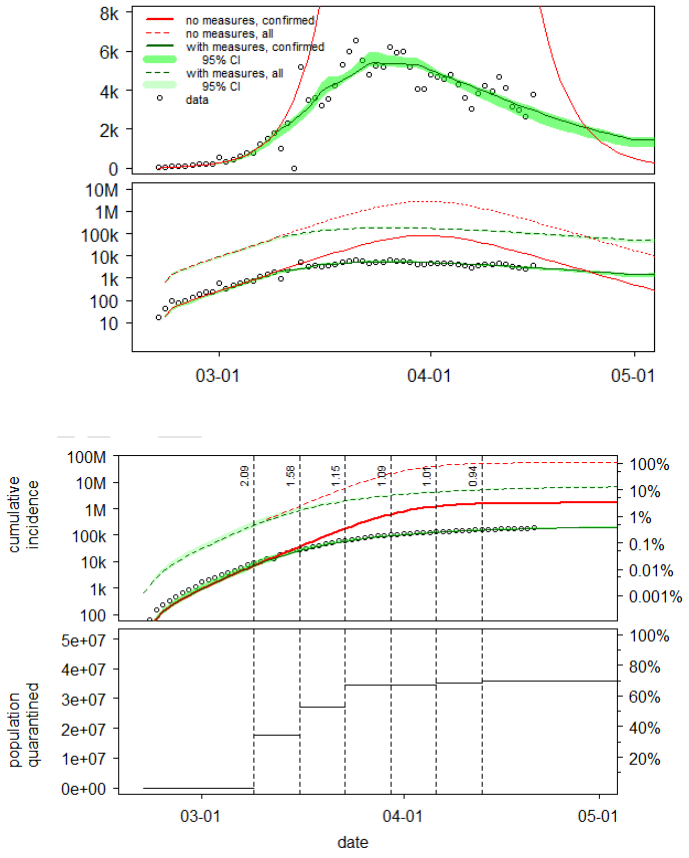

Fig. 3. Upper two panels: Linear and semi-log plots of daily incidence data of confirmed cases in Italy, together with maximum-likelihood model fit ("with measures, confirmed") and 95% CI envelope. Also shown is the inferred true number of infected, taking into account under-reporting and asymptomatic cases ("with measures, all"). Shown for comparison are the number of confirmed cases ("no measures, confirmed") and all cases ("no measures, all") expected to have occurred in the absence of countermeasures. **Lower two panels:** Cumulative incidence (top) and inferred week-by-week part of the susceptible population effectively quarantined (bottom).

It should again be emphasized that "percentage quarantined" represents an abstraction of the net effect of social distancing measures, rather than a quantity to be taken literally. Nevertheless, it provides a relatively interpretable measure of the week-by-week impact of social distancing/shelter-in-place measures on the normal functioning of society. Across the three countries, 40-70% of the susceptible population is inferred to be effectively quarantined by the third week of April.

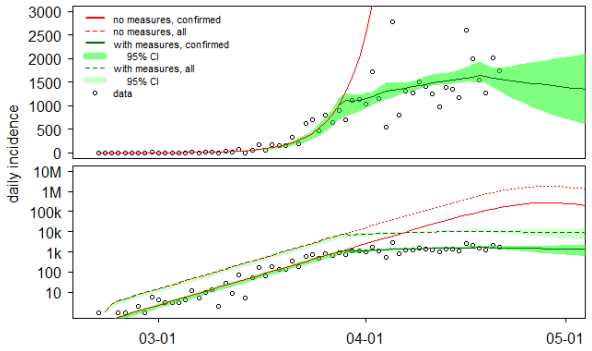

Fig. 4. Canadian daily COVID-19 incidence and maximum-likelihood model fit; see caption of Figure 3 for details

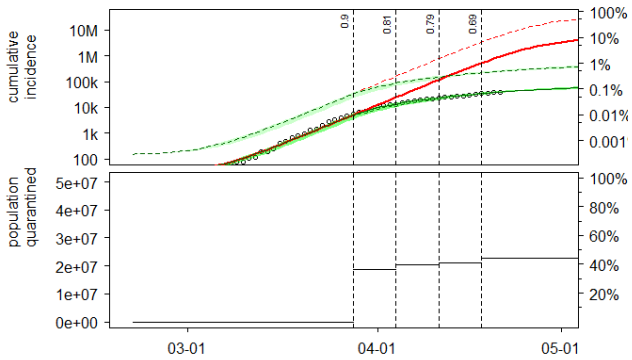

Fig. 5. Canadian cumulative incidence, model fit and inferred part of the population effectively quarantined; see caption of Figure 3 for details

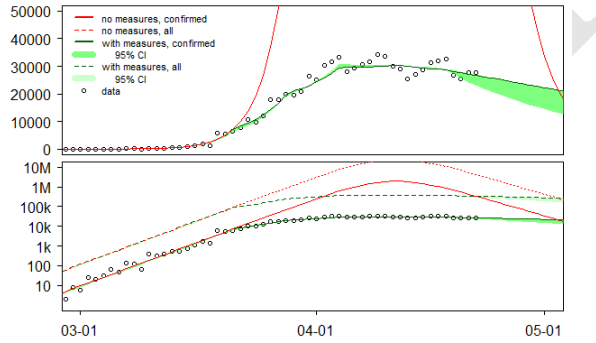

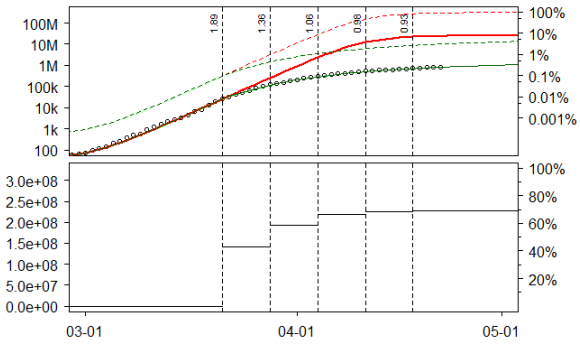

Fig. 6. U.S. daily COVID-19 data and model fit for incidence and cumulative incidence, and the inferred part of the population effectively quarantined; see caption of Figure 3 for details

C. Long-term prospects with social distancing alone. As an example, we evolve Italy forward in time. The currently-inferred level of effective quarantine, 70%, is kept in place until 1 June 2020, by which time daily incidence is predicted to have dropped to a level of several hundred cases per day. From that point forward, we make monthly adjustments to the effective quarantine level in order to maintain $R_{eff} \approx 1$. Results are shown in Figure 7. This allows reducing the quarantined population to about 60%. However, thereafter the quarantined can only be released extremely slowly if R_{eff} is to remain at 1. This is because, at a rate of several hundred cases per day, only a very small fraction of the pool of susceptibles is removed each day. Under this scenario, we predict that the quarantined fraction of susceptibles in Italy would still need to be about 55% even by the end of 2021.

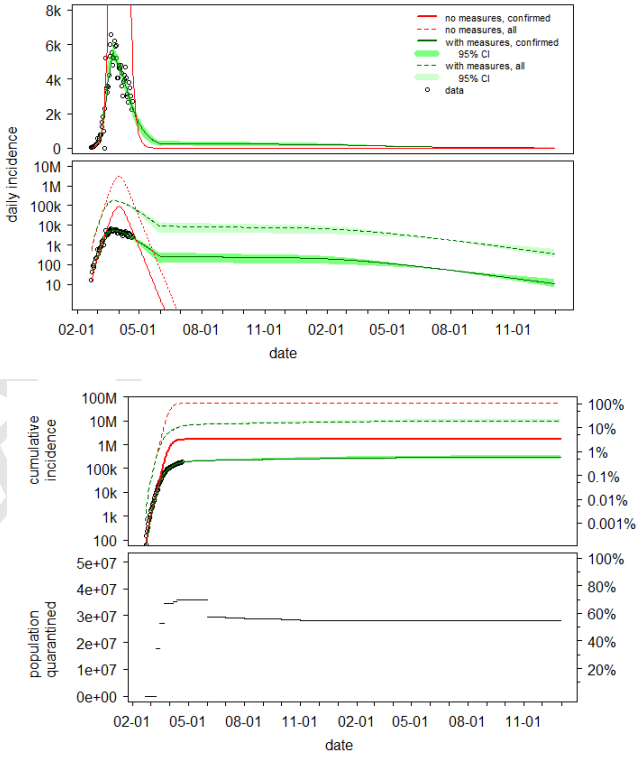

Fig. 7. Modeling the release of the the effectively-quarantined population of Italy from 1 June 2020 onward, while keeping $R_{eff} \approx 1$ in order to prevent further outbreak waves.

D. Large-scale testing and contact tracing - the case of South Korea. As we have seen in the previous section, South Korea experienced a very similar early exponential growth in cases, and hence has a similar inferred R_0, as the other three countries. However, its mitigation and control measures have differed substantively. The country employed a rapid scale-up of testing, concurrent with contact tracing and isolating of infected individuals. There are social distancing measures imposed, but no shelter-in-place, which is the main difference in this region. The population has not only agreed, but volunteered to participate in a continual surveillance of contacts in order to identify potential spread early.

In reproducing South Korea's daily case counts with the S(Q)EIRL model, we accordingly allow for some quarantining

(approximately 1/3 of the level in Italy in the corresponding intervention week). We now fit the values of the isolation rates of latent and infectious individuals, κ_1 and κ respectively, where we impose $\kappa_1 = \kappa$ for simplicity. Results are shown in Figure 8. We can see that for most of the weeks, the inferred effective time to isolation remains below 5 days.

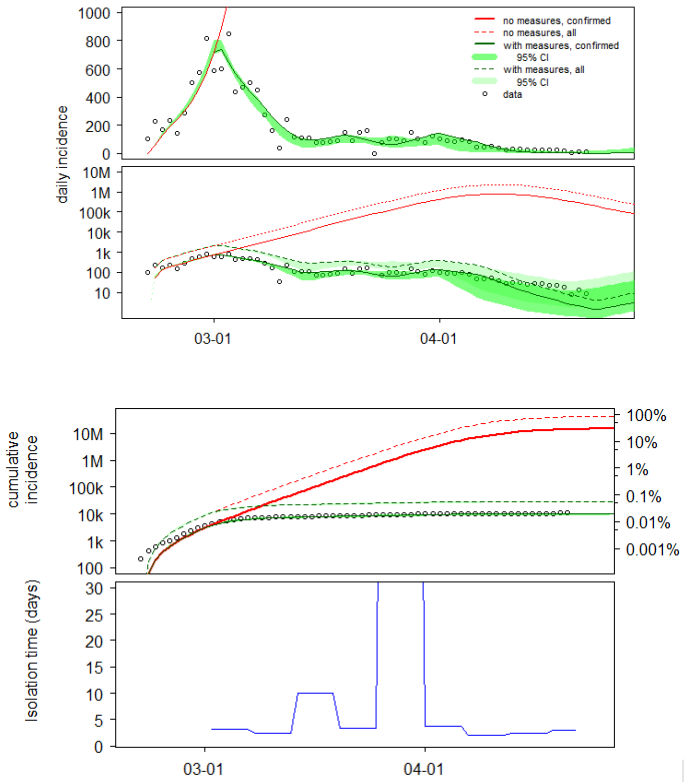

Fig. 8. South Korea short term

4. Continuous universal testing and contact tracing as a pathway out of social distancing

For a given set of values of β, σ and γ, Equation 9 gives us $R_{eff,S(Q)EIRL}$ as a function of κ and κ_1. This relationship is depicted as a surface plot in Figure (9) for $\sigma = \gamma = \frac{1}{2.5}$ and $\sigma = \gamma = \frac{1}{5}$. In the latter case, $R_{eff,S(Q)EIRL}$ is nearly twice as large as in the former. It is interesting to note, though, that for both cases, the combinations of κ and κ_1 that make $R_{eff,S(Q)EIRL} = 1$ (i.e. the intersections of the respective surfaces with the $R_0 = 1$ plane) are quite similar. This can be understood as follows: As σ and γ become small compared to κ_1 and κ, respectively, it is the latter which increasingly dominate the rate at which exposed/infected people are removed.

From Equation 9, we obtain the relationship between κ and κ_1 that makes $R_{eff,S(Q)EIRL} = 1$

$$1 = \frac{s\beta\sigma}{(\sigma+\kappa_1)(\gamma+\kappa)} \implies k = \frac{s\beta\sigma}{\sigma+\kappa_1} - \gamma$$

Extracting the current values of s from our simulated countries, we then compute the needed testing rates to achieve an effective reproduction number of 1 and present them compactly in the next table

Fig. 9. Effects of isolation rates due to testing and contact tracing on the initial value of $R_{0S(Q)EIRL}$ model. We computed $\sigma = \gamma = \frac{1}{2.5}$ (upper most surface), $\sigma = \gamma = \frac{1}{5}$ (middle surface) and the reference surface $R_0 = 1$.

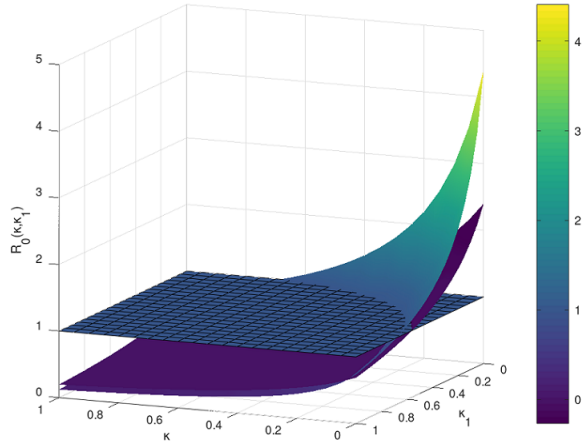

	β	s	κ $\kappa_1 = 0$	$\frac{1}{\kappa}$	$\kappa = \kappa_1$	$(\frac{1}{\kappa}, \frac{1}{\kappa_1})$
Italy	1.024	0.89	0.51	2 days	0.2	(5,5) days
Can	0.9925	0.99	0.58	1.72 days	0.23	(4.34,4.34) days
US	1.332	0.9	0.8	1.16 days	0.31	(3.125, 3.125) days
SK	0.961	0.999	0.56	1.78 days	0.22	(4.5, 4.5) days

Table 2. In all cases, we chose $\gamma = \sigma = \frac{1}{2.5}$ for a $T_{ser} = 5$ days and where s are the estimated values of susceptibles remaining in each country in the beginning of June 2020.

We present next pandemic forecasts under different testing and contact tracing rates, in the four countries under consideration. In Figure 10 below, we clearly see that for values of κ^{-1} and κ_1^{-1} shorter than the thresholds given in Table 2, a second pandemic wave is averted in each respective country. This threshold is the least stringent in Italy, where about 10% of the population (accounting for asymptomatic

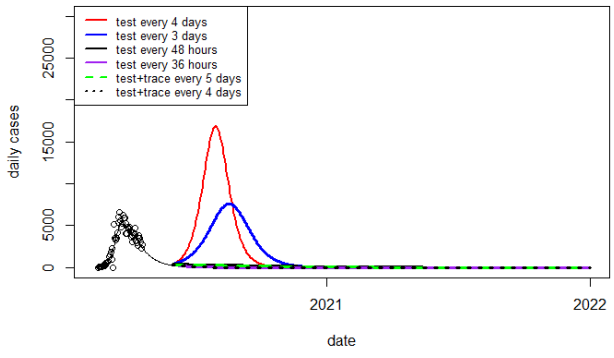

Fig. 10. Predicted daily cases in Italy under different rates of isolation due to testing, or testing plus contact-tracing, accompanied by a cessation of distancing measures accompanied by different with various isolation rates due to testing only, or a combination of testing and contact tracing

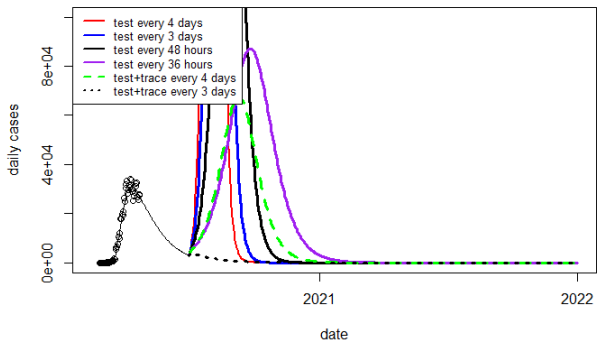

Fig. 11. Predicted daily cases in the U.S. under different rates of isolation due to testing, or testing plus contact-tracing, accompanied by a cessation of distancing measures.

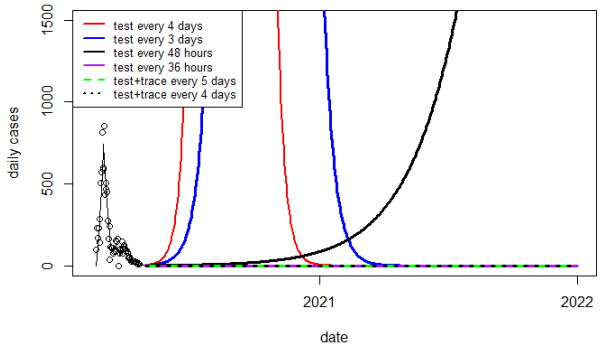

Fig. 13. Predicted daily cases in the South Korea under different rates of isolation due to testing, or testing plus contact-tracing, accompanied by a cessation of distancing measures.

and/or unreported cases) is inferred to have been infected in the first wave. It is the most stringent for the U.S., where the value of R_0 inferred from the initial exponential rise of cases is significantly higher than that of the other three countries. Some caution is warranted, though, since the initial rise of cases in the U.S. may have been partially enhanced by the initially poor testing capacity ramping up at the same time.

We depict here the Canada and South Korea in several respective testing and contact tracing scenarios:

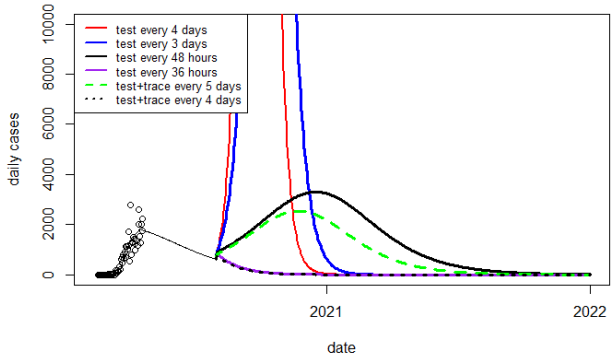

Fig. 12. Predicted daily cases in the Canada under different rates of isolation due to testing, or testing plus contact-tracing, accompanied by a cessation of distancing measures.

5. Discussion

In keeping with other published findings for these and other countries, our results suggest that the COVID-19 countermeasures taken in South Korea, Italy, Canada and the United States have had a substantial impact on the course of the disease. Even accounting for estimated under-reporting, the number of cases in these countries appears thus far to have been suppressed by roughly an order of magnitude in Italy and the US, two orders of magnitude in Canada, and three orders of magnitude in South Korea. The development of effective vaccines and treatments will be critical to the future control of this disease, however in the interim, non-pharmaceutical interventions are the only recourse.

Modeling studies unanimously show that, barring a proportion of asymptomatic cases so large that the majority of people have already been infected, a second wave of disease is inevitable if distancing measures are fully halted. We show that a "slow-burn" approach of gradually relaxing measures while avoiding subsequent outbreaks requires an infeasibly long time; even by the end of 2021, such measures would still need to be in force at a level equivalent to quarantining roughly half of the population.

The example of South Korea has successfully demonstrated (so far at least) an alternate hybrid strategy, in which a massive nationwide program of testing and contact tracing allows society to avoid a complete shutdown, albeit with extensive protective measures in place. In this work, we have attempted to quantify the level of testing which would be needed to allow a country to make a near-complete return to a normal functioning of its society. Among the countries considered here, we estimate that a strategy of universal testing alone would require an average testing frequency ranging from about once every 48 hours (Italy) to once a day (the U.S.) for every person. If testing is combined with contact-tracing, and/or if testing is able to already detect infections in their latent phase, then a testing rate ranging from once every 5 days (Italy) to once every 3 days (the U.S.) would be sufficient. These estimates assume a test with sensitivity at or near 100% and immediate isolation once a subject tests positive. Though reaching these targets would necessitate an undeniably enormous logistic effort, the prospect of an indefinitely-prolonged global shutdown is more daunting still. Furthermore, South Korea has demonstrated (and is continuing to do so) that such an exercise is far from impossible. Assuming social distancing at about a third the level of Italy, we infer an effective mean isolation time well below 5 days from 1 April 2020 onward in South Korea. Development and universal distribution of a self-testing solution combined with further advances in mobile device-based contact tracing would bring a testing-based exit strategy from global quarantine even closer. Nevertheless, it is vital not to rush into a relaxing of distancing measures. First, testing capacity and strong sustainable supply chains for delivery of tests and results must be built. Second, as illustrated in Figures 10 to 13, if a change in control strategy causes R_{eff} to exceed 1, how quickly a second wave builds depends on the number of cases at that time. South Korea

has few cases, so (slightly) exceeding $R_{eff} = 1$ would result in a gradual climb of cases, whereas doing so in Canada, which in the near term is predicted to have a significantly higher incidence, would cause a more rapid second wave. Given the uncertainty of how things will actually play out under a new set of strategies, it is important for countries to not experiment lightly with relaxing quarantine measures until they have a daily number of infected cases well under control, in order to give themselves reaction time in case things devolve towards a second wave.

Our work is subject to a number of limitations. We are simulating large, heterogeneous, geographically widely-distributed populations with an unstratified disease transmission model. Although we have taken the proportion of asymptomatic COVID-19 cases to be 50%, informed by mass-testing results in Iceland, this number is quite uncertain and may in fact be substantially higher; a recently-published seroprevalence study found the number of COVID-19 seropositives in to be 50- to 80-fold higher than the confirmed cases in a study population drawn from Santa Clara County, California (27). Assuming asymptomatic infection confers immunity, this would mean a smaller remaining pool of susceptibles and thus a lower current effective reproduction number. Estimates of R_0 from time series data of cases depend, as always, on the assumed latent and infectious periods. As we have demonstrated, though (Figure 9), if these periods are longer than the isolation time, then it is the latter which principally drives the disease dynamics. Thus, our findings about threshold isolation times are relatively robust against the possibility of a substantially longer COVID1-9 serial interval.

6. Conclusion

Both quarantine and testing and tracing policy directions will have to have a very strong dependability on the public cooperation and compliance. In the first policy, prolonged quarantine and slow relaxation has an unsustainable economic, as well as social and psychological, toll. Populations will become anxious to resume more normal work, school and social schedules, while compliance with strict measures will become harder to enforce. Under the latter policy, the population is needed to be relied on to comply with self-isolation if testing positive for the virus, as well as self-isolation upon being exposed to an infected person. Last but not least, sustainable supply chains, accuracy and reliability of possible tests as well as privacy issues around electronic contact tracing technology all present important, though not insurmountable, hurdles countries have to come to solve. On the side-by-side comparison here, the testing and tracing policy is clearly much more desirable and should be the one to strive for in the immediate short-term.

A. Appendix

A. Local exponential growth around a disease free equilibrium with $s(0) \leq 1$ in an S(Q)EIRL model. We want to find a relation between the exponential growth of the infected compartment in an SEIRL model (9) and the reproductive number R_0 around a disease-free equilibrium of the type $(s(0) = \tilde{s} \leq 1, 0, 0, 0)$ which arises as a possibility in a first wave $(\tilde{s} = 1)$ or a second wave of a pandemic such as COVID-19 $(\tilde{s} < 1)$.

In this case, we conduct a similar computation as in (13), but considering the 4 dimensional system of equations for s, e, i, l leads us to the Jacobian of the S(Q)EIRL:

$$J = \begin{pmatrix} -\beta i & 0 & -\beta s & 0 \\ \beta i & -(\sigma+\kappa_1) & \beta s & 0 \\ 0 & \sigma & -(\gamma+\kappa) & 0 \\ 0 & 0 & \kappa & 0 \end{pmatrix}.$$

If computed at the disease free equilibrium $(\tilde{s}, 0, 0, 0)$ we further obtain:

$$J = \begin{pmatrix} 0 & 0 & -\beta\tilde{s} & 0 \\ 0 & -(\sigma+k_1) & \beta\tilde{s} & 0 \\ 0 & \sigma & -(\gamma+\kappa) & 0 \\ 0 & 0 & \kappa+\kappa_1 & 0 \end{pmatrix}.$$

Again we note that the linearized equations for s and l are decoupled from the equations of e and i, thus, to get information on the growth rate of the infected compartment, let us try to solve the linearized reduced system in (e, i) based on the reduced Jacobian:

$$J_{reduced} = \begin{pmatrix} -(\sigma+\kappa_1) & \beta\tilde{s} \\ \sigma & -(\gamma+k) \end{pmatrix} \overset{Solve:}{\Longrightarrow} det(\rho I_2 - J_{reduced}) = 0$$

Its characteristic equation is:

$$\rho^2 - \rho((\sigma+\kappa_1)+(\gamma+\kappa)) + (\sigma+\kappa_1)(\gamma+\kappa) - \sigma\beta\tilde{s} = 0$$

The eigenvalues of this matrix can be computed to be

$$\rho_{1,2} = \frac{-(\sigma+\kappa_1+\gamma+\kappa)}{2} \pm \frac{\sqrt{(\sigma+\kappa_1+\gamma+\kappa)^2 - 4((\sigma+\kappa_1)(\gamma+\kappa) - \sigma\beta\tilde{s})}}{2} \Leftrightarrow$$

$$\rho_{1,2} = \frac{-(\sigma+\kappa_1+\gamma+\kappa) \pm \sqrt{((\sigma+\kappa_1)-(\gamma+\kappa))^2 + 4\sigma\beta\tilde{s}}}{2} \quad [13]$$

We first note that $((\sigma+\kappa_1)-(\gamma+\kappa))^2 + 4\sigma\beta\tilde{s} > 0$, given all parameters are positive. This implies that $\rho_1 \neq \rho_2 \in \mathbb{R}$ and clearly $\rho_2 < 0$. We check whether $\rho_1 > 0$ by looking at

$$\sqrt{((\sigma+\kappa_1)-(\gamma+\kappa))^2 + 4\lambda\beta\tilde{s}} > \sigma+\kappa_1+\gamma+\kappa \Leftrightarrow$$

$$(\sigma+\kappa_1)-(\gamma+\kappa))^2 + 4\lambda\beta\tilde{s} > ((\sigma+\kappa_1)+(\gamma+\kappa))^2 \Leftrightarrow$$

$$-2(\sigma+\kappa_1)(\gamma+\kappa) + 4\sigma\beta\tilde{s} > 2(\sigma+\kappa_1)(\gamma+\kappa) \implies$$

$$\sigma\beta\tilde{s} > (\sigma+\kappa_1)(\gamma+\kappa) \Leftrightarrow \beta\tilde{s} > \frac{(\sigma+\kappa_1)(\gamma+\kappa)}{\sigma\beta}$$

Therefore, as before, we have that

$$\rho_1 > 0 \text{ as long as } \tilde{s} > \frac{(\sigma+\kappa_1)(\gamma+\kappa)}{\sigma\beta} \quad [14]$$

Inequality (14) simply shows that in order to not have an exponential growth from our disease free equilibrium (in other words the infection dies out), we need to allow that the initial fraction of susceptibles is lower than

$$\tilde{s} \leq \frac{(\sigma+\kappa_1)(\gamma+\kappa)}{\sigma\beta}$$

We note that β and γ are disease-dependent values on which we cannot exert control. However, κ and κ_1 are parameters on which we can exert an exogenous control (specifically to increase them, thus raising the upper bound on fractions $\tilde{s}$ with no exponential growth in infected) which will be outlined in detail in the next section.

Continuing as in (13), we express β as a function of $\tilde{s}, \sigma, \gamma, \kappa, \kappa_1$ from (13) and we get:

$$2\rho_1+(\sigma+\kappa_1)+(\gamma+\kappa) = \sqrt{((\sigma+\kappa_1)-(\gamma+\kappa))^2+4\sigma\beta\tilde{s}} \implies$$

$$4\rho_1^2+(\sigma+\kappa_1)^2+2(\sigma+\kappa_1)(\gamma+\kappa)+(\gamma+\kappa)^2+4\rho_1(\sigma+\kappa_1)+4\rho_1(\gamma+\kappa) =$$

$$(\sigma+\kappa_1)^2-2(\sigma+\kappa_1)(\gamma+\kappa)+(\gamma+\kappa)^2+4\sigma\beta\tilde{s} \iff$$

$$4\rho_1^2+4(\sigma+\kappa_1)(\gamma+\kappa)+4\rho_1(\sigma+\kappa_1)+4\rho_1(\gamma+\kappa) = 4\sigma\beta\tilde{s} \implies$$

$$\frac{\rho_1^2+(\sigma+\kappa_1)(\gamma+\kappa)+\rho_1(\sigma+\kappa_1)+\rho_1(\gamma+\kappa)}{\sigma\tilde{s}} = \beta \iff$$

$$\frac{(\sigma+\kappa_1+\rho_1)(\gamma+\kappa+\rho_1)}{\sigma\tilde{s}} = \beta$$

Following (28), we can use the next generation matrix to deduce R_0 as the dominant eigenvalue of the next generation matrix:

$$FV^{-1} = \begin{pmatrix} \frac{\beta\sigma\tilde{s}}{(\sigma+\kappa_1)(\gamma+\kappa)} & \frac{\beta\tilde{s}}{\gamma+\kappa} \\ 0 & 0 \end{pmatrix} \implies R_0 = \frac{\beta\sigma\tilde{s}}{(\sigma+\kappa_1)(\gamma+\kappa)}$$

Now using the expression of β in that of R_0 we are able to express the effective reproductive number as a function of the exponential growth and of γ, σ, κ, κ_1:

$$R_0 = \frac{\sigma\tilde{s}}{(\sigma+\kappa_1)(\gamma+\kappa)}\frac{(\sigma+\kappa_1+\rho_1)(\gamma+\kappa+\rho_1)}{\sigma\tilde{s}} \implies$$

$$R_0 = \frac{(\sigma+\kappa_1+\rho_1)(\gamma+\kappa+\rho_1)}{(\sigma+\kappa_1)(\gamma+\kappa)} \text{ and } R_{eff} = s(t)R_0,\ \forall t > 0$$

Similar to (7) we denote by $R_{0S(Q)EIRL}$:

$$R_{0S(Q)EIRL} = \frac{(\sigma+\kappa_1+\rho_1)(\gamma+\kappa+\rho_1)}{(\gamma+\kappa)\sigma}$$

Clearly, if $\kappa = \kappa_1 = 0$ then $R_{0S(Q)EIRL}$ reduces to R_{0SEIR} in (7) of Section 2.

Let us now note that we have shown that the exponential growth factor (13), as well as the $R_{0S(Q)EIRL}$, are dependent on the rates κ and κ_1, that is to say, we denote by

$$\rho(\kappa,\kappa_1) = \frac{-(\sigma+\kappa_1+\gamma+\kappa)+\sqrt{((\sigma+\kappa_1)-(\gamma+\kappa))^2+4\sigma\beta\tilde{s}}}{2},$$

$$\text{and by } R_0(\kappa,\kappa_1) = \frac{(\sigma+\kappa_1+\rho_1)(\gamma+\kappa+\rho_1)}{(\gamma+\kappa)\sigma}$$

B. The reproductive number as a function of T_{lat}. Let us express the reproductive number, in general, as a function of $T_{lat} = \frac{1}{\sigma}$ and $T_{ser} = T_{inf} + T_{lat} = \frac{1}{\gamma} = T_{ser} - T_{lat} \implies \gamma = \frac{1}{T_{ser}-T_{lat}}$.

From 7 we have that

$$R_0 = \frac{(\rho+\gamma)(\rho+\sigma)}{\gamma\sigma} = \frac{(\rho+\frac{1}{T_{lat}})(\rho+\frac{1}{T_{ser}-T_{lat}})}{\frac{1}{T_{lat}(T_{ser}-T_{lat})}}$$

$$= (\rho T_{lat}+1)(\rho(T_{ser}-T_{lat})+1).$$

Then

$$R_0 = -(T_{lat}\rho - T_{ser}\rho - 1)(T_{lat}\rho+1) \implies$$

$$\frac{dR}{dT_{lat}} = -\rho(T_{lat}\rho+1)-(T_{lat}\rho-T_{ser}\rho-1)\rho$$

where we can solve for a T_{lat} value which maximizes R_0, namely

$$\frac{dR}{dT_{lat}} = 0 \iff -2T_{lat}\rho + T_{ser}\rho \implies T_{lat} = \frac{T_{ser}}{2}.$$

ACKNOWLEDGMENTS. M. G. Cojocaru acknowledges support from the National Science and Engineering Research Council of Canada, Discover Grant 400684 (PI: Cojocaru).

1. Q Li, et al., Early transmission dynamics in wuhan, china, of novel coronavirus–infected pneumonia. *New Engl. J. Medicine* **0**, null (0).
2. C Anastassopoulou, L Russo, A Tsakris, C Siettos, Data-based analysis, modelling and forecasting of the novel coronavirus (2019-ncov) outbreak. *medRxiv* (2020).
3. RA Neher, R Dyrdak, V Druelle, EB Hodcroft, J Albert, Potential impact of seasonal forcing on a sars-cov-2 pandemic. *medRxiv* (2020).
4. SA Lauer, et al., The Incubation Period of Coronavirus Disease 2019 (COVID-19) From Publicly Reported Confirmed Cases: Estimation and Application. *Annals Intern. Medicine* (2020).
5. YR Gau, et al., The origin, transmission and clinical therapies on coronavirus disease 2019 (COVID-19) outbreak – an update on the status. *Mil. Med. Res.* (2020).
6. K Mizumoto, K Kagaya, G Chowell, Early epidemiological assessment of the transmission potential and virulence of coronavirus disease 2019 (covid-19) in wuhan city: China, january-february, 2020. *medRxiv* (2020).
7. AR Tuite, et al., Estimation of covid-2019 burden and potential for international dissemination of infection from iran. *medRxiv* (2020).
8. RM Centor, DN Fisman, Annals on call-understanding the spread of covid-19. *Annals Intern. Medicine*, OC1–OC1 (2020).
9. A Tuite, V Ng, E Rees, D Fisman, Estimation of covid-19 outbreak size in italy based on international case exportations. *medRxiv* (2020).
10. LDea Ferguson N. M, Impact of non-pharmaceutical interventions (npis) to reduce covid-19 mortality and healthcare demand. *medRxiv* (2020).
11. SM Kissler, C Tedijanto, E Goldstein, YH Grad, M Lipsitch, Projecting the transmission dynamics of sars-cov-2 through the postpandemic period. *Science* (2020).
12. WO Kermack, AG McKendrick, A contribution to the mathematical theory of epidemics. *Proc. royal society london. Ser. A, Containing papers a mathematical physical character* **115**, 700–721 (1927).
13. J Ma, Estimating epidemic exponential growth rate and basic reproduction number. *Infect. Dis. Model.* (2020).
14. F Brauer, The kermack–mckendrick epidemic model revisited. *Math. biosciences* **198**, 119–131 (2005).
15. E Dong, H Du, L Gardner, An interactive web-based dashboard to track covid-19 in real time. *The Lancet Infect. Dis.* (2020).
16. D Cereda, et al., The early phase of the covid-19 outbreak in lombardy. *Italy.. arXiv* **2003** (2020).
17. T Ganyani, et al., Estimating the generation interval for covid-19 based on symptom onset data. *medRxiv* (2020).
18. L Tindale, et al., Transmission interval estimates suggest pre-symptomatic spread of covid-19. medrxiv. *Prepr. doi* **10**, 03–20029983 (2020).
19. Q Bi, et al., Epidemiology and transmission of covid-19 in shenzhen china: Analysis of 391 cases and 1,286 of their close contacts. *MedRxiv* (2020).
20. DGJ McNeil, The virus can be stopped, but only with harsh measures, experts say. *The New York Times* (2020).
21. F D'Emilio, Europe hopeful as italy's daily coronavirus death toll falls to lowest in weeks. *The Assoc. Press.* (2020).
22. C News, Coronavirus: Here's what's happening on march 22. *CBC News* (2020).
23. P Alvarez, Here's what trump's coronavirus emergency declaration does. *CNN* (2020).
24. Using a delay-adjusted case fatality ratio to estimate under-reporting (https://cmmid.github.io/topics/covid19/severity/global_cfr_estimates.html) (2020) Accessed: 2020-04-19.

25. Iceland lab's testing suggests 50% of coronavirus cases have no symptoms (https://www.cnn.com/2020/04/01/europe/iceland-testing-coronavirus-intl/index.html) (2020) Accessed: 2020-04-19.
26. G Cowan, *Statistical data analysis.* (Oxford university press), (1998).
27. E Bendavid, et al., Covid-19 antibody seroprevalence in santa clara county, california. *medRxiv* (2020).
28. P van den Driessche, Reproduction numbers of infectious disease models. *Infect. Dis. Model.* **2**, 288–303 (2017).